PHOTONIC SENSORS / Vol. 4, No. 3, 2014: 193–197

Temperature Insensitive Bending Sensor Based on In-Line Mach-Zehnder Interferometer

Xue CHEN[1], Yongqin YU[2*], Xiaomei XU[2], Quandong HUANG[1], Zhilong OU[1], Jishun WANG[1], Peiguang YAN[1], and Chenlin DU[1]

[1]*College of Electronic Science and Technology, Shenzhen University, Shenzhen, 518060, China*

[2]*College of Physics Science and Technology, Shenzhen Key Laboratory of Sensor Technology, Shenzhen University, Shenzhen, 518060, China*

[*]Corresponding author: Yongqin YU E-mail: yuyq@szu.edu.cn

Abstract: A simple and compact fiber bending sensor based on the Mach-Zehnder interferometer was proposed. A photonic crystal fiber (PCF) with a length of 10 mm was spliced by collapsing air holes with two conventional single mode fibers to consist of an all fiber bending sensor. The sensitivity of 0.53 nm/m^{-1} was obtained at 1586 nm for the curvature range from 0 to 8.514 m^{-1}. The temperature sensitivity was very low. The measurement error due to the temperature effect was about 8.68×10^{-3} m^{-1}/℃, and the temperature effect in the curvature measurement could be ignored. This device can avoid the cross sensitivity of the temperature in the curvature measurement.

Keywords: Photonic crystal fiber, Mach-Zehnder interferometer, bending sensor

Citation: Xue CHEN, Yongqin YU, Xiaomei XU, Quandong HUANG, Zhilong OU, Jishun WANG, *et al*., "Temperature Insensitive Bending Sensor Based on In-Line Mach-Zehnder Interferometer," *Photonic Sensors*, 2014, 4(3): 193–197.

1. Introduction

Optic fiber bending sensors owing to the unique advantages, for instance, the high sensitivity, good physical stability, and low cost, have been used and developed in many fields, such as the structural deformation, intelligent artificial limb, and mechanical engineering. H. P. Gong *et al*. presented a curvature sensor by using the low-birefringence photonic crystal fiber (PCF) based Sagnac loop in 2010, they achieved the sensitivity of the curvature was 0.337 nm/m^{-1} for the bending rang change from 0 to 9.9 m^{-1}, and the temperature sensitivity was about 0.125 nm/℃. Among the bending sensors, the bending sensors based on the Mach-Zehnder interferometer (MZI) possess the advantages such as the production process is simple and the structure is compact [1]. The MZI have been commonly made of an optical fiber and two optical fiber mode couplers. There are many different methods to achieve the MZI structure, such as fiber core mismatch splicing [2–4], a pair of LPFGs [5–7], and air-hole collapsing of a PCF [8–10]. Our research group, Zhilong Ou *et al*., proposed a bending vector sensor based on the seven-core PCF using lateral offset splicing, we obtained the maximum curvature sensitivity was 1.232 nm/m^{-1}, and the temperature sensitivity was 0.011 nm/℃ [11]. The bending sensors reported before were usually sensitive to the temperature.

In this paper, we use a simple method collapsing air holes of an index-guiding PCF to achieve a PCF

Received: 26 November 2013 / Revised version: 11 December 2013

DOI: 10.1007/s13320-013-0156-x
Article type: Regular

MZI. The PCF with a length of 10 mm was spliced with collapsing air holes between two single mode fibers (SMFs). Because of the structure of air holes in the PCF, the interference was induced only by core modes rather than cladding modes in the PCF. We achieved a temperature insensitive bending sensor based on the PCF-MZI, and the bending sensitivity was 0.53 nm/ m^{-1} at 1586 nm for the curvature range from 0 to 8.514 m^{-1}. These sensitivities were higher than that of the Sagnac loop-based curvature sensor (0.337 nm/m^{-1}) [1]. When the temperature changed from 30 ℃ to 120 ℃, the wavelength variation was about 0.46 nm at 1520 nm, and the sensitivity was small enough to be ignored.

2. Experimental setup and principle

In our experiment, the PCF cross sectional view is shown in Fig. 1(b), the diameter of the pure-silica core was about 5.63 μm, and the air holes with diameter of 2.59 μm were arranged in seven layers. The pitch between two air holes was 3.98 μm, and the cladding diameter was about 125 μm.

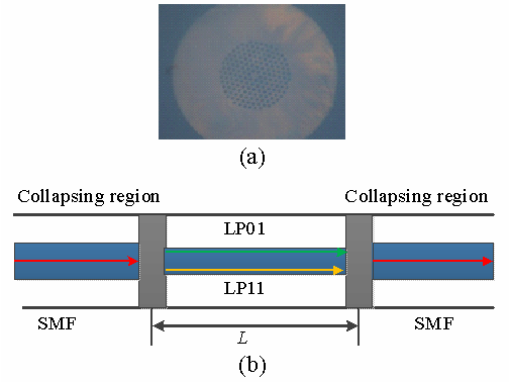

Fig. 1 Cross section of the PCF and schematic of the PCF-MZI: (a) cross section of the PCF and (b) schematic of the PCF-MZI consisting of two series-wound collapsing regions of the PCF.

Figure 1(a) shows the schematic of the PCF-MZI consisting of two series-wound collapsing regions of the PCF. When the light is spread into the first collapsing region, the higher order mode is excited, a strong mode coupling occurs, and the light energy is coupled from the fundamental mode to the higher order mode. While the high order mode is re-coupled back to the fundamental mode at the second collapsing region, the interference happens in the MZI, and the total intensity can be given by

$$I(\lambda) = I_1(\lambda) + I_2(\lambda) + 2\sqrt{I_1(\lambda) I_2(\lambda)} \cos(\frac{2\pi \Delta n_{\text{eff}} L}{\lambda}) \tag{1}$$

where $I_1(\lambda)$ and $I_2(\lambda)$ are the powers of two interference modes at the wavelength of λ, L is the length of the MZI, and Δn_{eff} is the effective index difference of the two modes, which is defined as

$$\Delta n_{\text{eff}} = n_{\text{eff}}^{\text{core}} - n_{\text{eff}}^{\text{HOM}} \tag{2}$$

where $n_{\text{eff}}^{\text{core}}$ and $n_{\text{eff}}^{\text{HOM}}$ represent the effective mode refractive indices of the fundamental mode and the high order mode, respectively.

At the second collapsing region, the phase difference generated in the PCF between the two modes can be defined as

$$\Delta \phi^m = 2\pi \Delta n_{\text{eff}} L / \lambda_m . \tag{3}$$

Transmission dips appear only when phase matching is satisfied with $\Delta \phi^m = (2m+1)\pi$. We can obtain

$$\lambda_m = \frac{(n_{\text{eff}}^{\text{core}} - n_{\text{eff}}^{\text{HOM}})L}{(2m+1)} \tag{4}$$

where m is any integer, and λ_m is the resonance dip wavelength. With the change in the curvature of the fiber, the optical path difference between the two modes will change, and it will induce the shift of the dip wavelength. We can measure the fiber curvature by measuring the shift of the dip wavelength.

Figure 2(a) shows the effective refractive of LP_{01} and like-LP_{11} as a function of the wavelength analyzed by the finite element method (FEM; COMSOL 3.5). According to Fig. 2, the effective refractive difference between the LP_{01} and like-LP_{11} mode is calculated to be $\Delta n_{\text{eff}} = 1.65 \times 10^{-2}$ at 1550 nm. The mode field distributions of LP_{01} and like-LP_{11} are shown in Fig. 2(b).

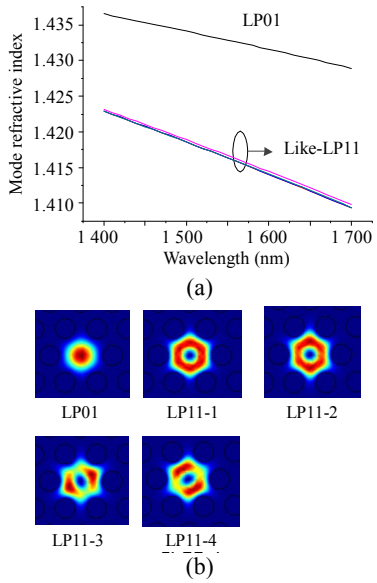

Fig. 2 Image of the effective mode refractive indices and the mode filed: (a) the effective mode refractive indices of LP_{01} and like-LP_{11} and (b) the mode filed contribution of LP_{01} and like-LP_{11} by the FEM.

3. Results and discussion

The experimental setup of the MZI for the bending sensor is shown in Fig. 3. The length of the PCF was 10 mm, A broad-band super luminescent light-emitting diode (SLD) optical source (1250 nm – 1700 nm, B&A Technology SL3200, China) and an optical spectrum analyzer (YOKOGAWA AQ6370B) with the 0.02-nm spectral resolution were connected to the MZI to measure the transmission spectra as the curvature changes. The fiber including the PCF-MZI was attached to a 17.5-cm-length copper sheet. In order to avoid the influence of twist, only the two ends of the fiber were fixed at opposite ends of a copper sheet. The copper sheet was placed at the middle of two fixed holders. The distance between two holders was 170 mm. The fiber was bent by depressing the center of the copper sheet with a micrometer driver. So we could measure the curvature by the change in the displacement [11]. This device could ensure the fiber does not bend to any other orientation. The curvature (C) of the sensor is given by [13]

$$C = \frac{2d}{(d^2 + L^2)} \tag{5}$$

where d is the displacement at the center of the MZI, and L is the half of the distance between the two holders.

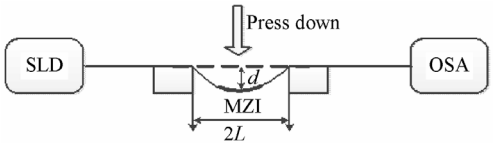

Fig. 3 Schematic diagram of the experimental setup for the bending sensor.

The transmission spectrum at the room temperature of the PCF MZI with the length of 10 mm is shown in Fig. 4. The high contrast ratio of the interference pattern was obtained to be more than 10 dB. The fringe period $\Delta\lambda$ was 14.13 nm at 1550 nm. At λ, the fringe period $\Delta\lambda$ of the MZI spectrum is determined by

$$\Delta\lambda = \frac{\lambda^2}{\Delta n_{\text{eff}} L}. \tag{6}$$

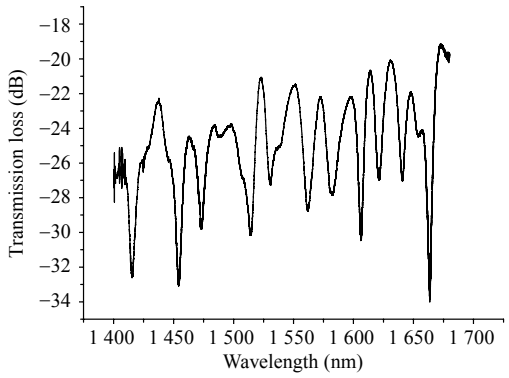

Fig. 4 Transmission spectrum of the sensor.

Using (6), the effective mode refractive indices difference Δn_{eff} between the fundamental mode and higher order mode around 1550 nm is calculated as $\Delta n_{\text{eff}} = 1.7 \times 10^{-2}$, which is almost consistent with the theoretical value ($\Delta n_{\text{eff}} = 1.65 \times 10^{-2}$) calculated by the FEM. It is indicated that the interference pattern is resulted from the phase difference generated in the PCF between the LP_{01} and like-LP_{11} modes.

Figure 5 shows the wavelength shift with an increase in the curvature in the curvature range from 2 m^{-1} to 8.514 m^{-1}. The bending sensitivity at 1586 nm was obtained to be 0.58 nm/m^{-1} by linear fitting.

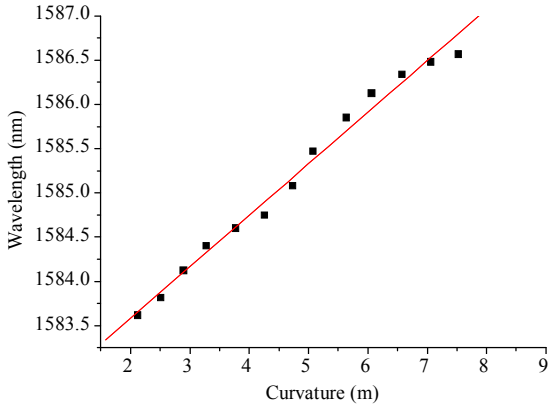

Fig. 5 Relationship of the curvature with the wavelength.

The MZI sensor was placed in a cylindrical heater oven to measure the temperature sensitivity in the temperature range from 30 ℃ to 120 ℃ with the step of 10 ℃. The dependence of the wavelength shift upon the temperature is shown in Fig. 6. We can observe that the wavelength shift is weakly dependent on the temperature, and the wavelength shift is less than 1 nm in the temperature range from 30 ℃ to 120 ℃. Compared with the maximum bending sensitivity, it is enough small to be ignored. So, we think the device can work as a temperature insensitive bending sensor.

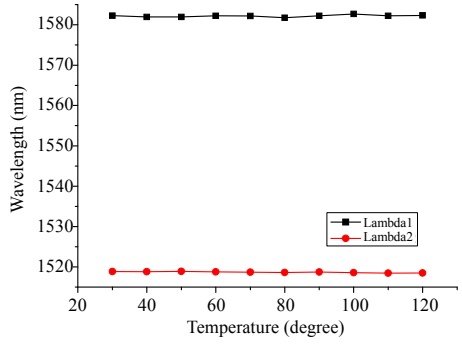

Fig. 6 Relationship of the wavelength shift with the temperature.

4. Conclusions

In summary, a bending sensor was achieved by using a PCF with the length of 10 mm fusion spliced with two SMFs. And the high sensitivity of bending at 1586 nm was obtained to be 0.53 nm/ m^{-1} in the curvature range of 2 m^{-1} to 8.514 m^{-1}. Moreover, the temperature sensitivity was relatively small, which ensured the MZI with the advantage of avoiding the crosstalk of the temperature in bending measurements. The fabrication process of the bending sensor that we proposed was simpler than that of the grating-based bending sensors, and the cost was low. It indicates that the device can be used as a temperature-independent bending sensor and has the potential for curvature sensing applications.

Acknowledgment

This work was supported by the National Natural Science Foundation of China (NSFC) under Grants No. 61275125, 61007054, 61308055, National High Technology Research and Development Program of China under Grant No. 2013AA031501 & 2012AA041203, Shenzhen Science and Technology Project (NO. JC201005280473A, JC201104210019A, ZDSY20120612094753264, JCYJ20130326113421781) and Specialized Research Fund for the Doctoral Program of Higher Education (SRFDP, 20124408120004).

References

[1] H. P. Gong, C. C. Chan, P. Zu, L. H. Chen, and X. Y. Dong, "Curvature measurement by using low-birefringence photonic crystal fiber based Sagnac loop," *Optics Communications*, 2010, 283(16): 3142–3144.

[2] J. R. Guzman-Sepulveda and D. A. May-Arrioja, "In-fiber directional coupler for high-sensitivity curvature measurement," *Optics Express*, 2013, 21(10): 11853–11861.

[3] X. Yu, P. Shum, and X. Dong, "Photonic-crystal-fiber-based Mac-Zehnder interferometer using long-period gratings," *Microwave And Optical Technology Letters*, 2006, 48(7): 1379–1383.

[4] C. Gouveia, P. A. S. Jorge, J. M. Baptista, and O. Frazao, "Temperature-independent curvature sensor using FBG cladding modes based on a core misaligned splice," *IEEE Photonics Technology Letters*, 2011, 23(12): 804–806.

[5] W. Shin, Y. L. Lee, B. A. Yu, Y. C. Noh, and T. J. Ahn, "Highly sensitive strain and bending sensor based on in-line fiber Mach-Zehnder interferometer in solid core large mode area photonic crystal fiber," *Optics Communications*, 2010, 283(10): 2097–2101.

[6] J. H. Lim, H. S. Jang, K. S. Lee, J. C. Kim, and B. H. Lee, "Mach-Zehnder interferometer formed in a photonic crystal fiber based on a pair of long-period fiber gratings," *Optics Letters*, 2004, 29(4): 346–348.

[7] Y. P. Wang and Y. J. Rao, "A novel long period fiber grating sensor measuring curvature and determining bend-direction simultaneously," *IEEE Sensors Journal*, 2005, 5(5): 839–843.

[8] W. C. Wong, C. C. Chan, H. Gong, and K. C. Leong, "Mach-Zehnder photonic crystal interferometer in cavity ring-down loop for curvature measurement," *IEEE Photonics Technology Letters*, 2011, 23(12): 795–797.

[9] J. Villatoro, V. P. Minkovich, V. Pruneri, and G. Badenes, "Simple all-microstructured-optical-fiber interferometer built via fusion splicing," *Optics Express*, 2007, 15(4): 1491–1496.

[10] J. Zheng, P. Yan, Y. Yu, Z. Ou, J. Wang, X. Chen, *et al*., "Temperature and index insensitive strain sensor based on a photonic crystal fiber in line Mach-Zehnder interferometer," *Optics Communications*, 2013, 297(15): 7–11.

[11] Z. Ou, Y. Yu, P. Yan, J. Wang, Q. Huang, X. Chen, *et al*., "Ambient refractive index-independent bending vector sensor based on seven-core photonic crystal fiber using lateral offset splicing," *Optics Express*, 2013, 21(20): 23812–23821.

[12] Y. Liu, J. A. R. Williams, and I. Bennion, "Optical bend sensor based on measurement of resonance mode splitting of long-period fiber grating," *IEEE Photonics Technology Letters*, 2000, 12(5): 531–533.

[13] H. J. Patrick, C. C. Chang, and S. T. Vohra, "Long period fiber gratings for structural bend sensing," *Electronics Letters*, 1998, 34(18): 1773–1775.